A.4 Data acquisition system for contact resistance measurement of superconducting corrector magnets

For the contact resistance (CR) measurement the magnet under test is charged with rated current. It is then taken to the persistence mode using a Superconducting -switch connected in parallel. The decay of the Hall voltage (placed inside the magnet), which is proportional to the current, is monitored, to calculate the CR of magnet. A micro-controller based online Data Acquisition System has been developed and GUI is made using Lab VIEW (fig. A.4.1). The system is based on digitally controlled analog 8-1 multiplexer. The Micro-controller is programmed to switch the multiplexer sequentially to acquire data from eight channels with required time. User configurable method of data acquisition system provides the user an option to select number of channels and the data is displayed and stored. The signal is directly acquired from the 6-½-digit multimeter using GPIB communication. Switching signal is generated from PC and communicated through RS-232 to Micro controller, which generate the switching through multiplexer. The user-friendly GUI display panel is designed which gives the direct display of CR.

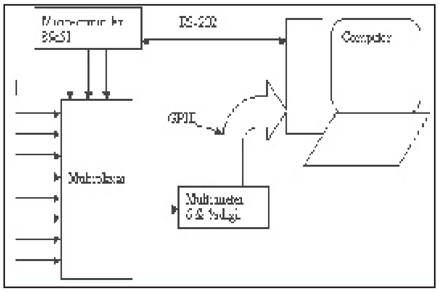

***Fig. A.4.1** DAS for contact resistance measurement*

(Contributed by: H. Ashoka, V P Singh and
A. M Puntambekar; avinash@cat.ernet.in)

A.5 Ferromagnetic shape memory alloys

Shape Memory Alloys (SMA) have gained considerable attention due to their technological importance as smart materials. The key factor for the shape memory effect is a diffusionless structural phase transition called martensitic transformation (MT), which occurs between a high temperature Austenite phase and a low temperature Martensite phase. Ferromagnetic shape memory alloys (FSMA) are ferromagnetically ordered materials exhibiting reversible MT. FSMA are important for realization of shape memory actuators as they show large strain (~10% in 1 Tesla field) and faster response when exposed to an external magnetic field as compared to the conventional temperature and/or stress induced SMA.

Our main goal in FSMA is to study the nature of the martensitic and magnetic transitions, which are the key to the shape memory effect. These studies are also fundamentally important for understanding the first-order nature of the solid-solid phase transition in metallic alloys. Presently we are working on few systems of alloys, *viz*. Ni- Fe-Ga, Ni-Co-Al and Co-Ni-Ga. The alloys are prepared by melting the constituent elements in an inert argon atmosphere. We investigated these FSMA by resistivity and ac susceptibility measurements. Although we are working on few different alloys, here we shall highlight our accepted work on $Ni_{54}Fe_{19}Ga_{27}$ alloy only (S. Majumdar *et al.*, Solid State Commun. in press).

Ni-Fe-Ga alloys have been recently reported to show magnetic shape memory effect. The composition $Ni_{54}Fe_{19}Ga_{27}$ is chosen for our study, because both the magnetic and martensitic transitions occur within the accessible temperature (*T*) range of measurements. The ferromagnetic transition temperature (T_C) of the alloy is found to be 290 K. In ac susceptibility (fig. A.5.1) and resistivity measurements, the alloy shows an anomalous feature around 220 K, which is associated with thermal irreversibility. We identify the feature around 220 K due to MT, which can show thermal hysteresis due to the first order nature of the phase transition. On the contrary, the paramagnetic-ferromagnetic transition at 290 K does not show any thermal hysteresis, as it is a second order phase transition.

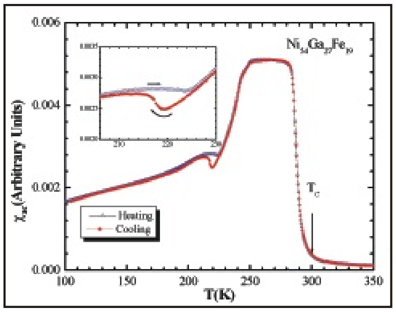

***Fig. A.5.1** Temperature dependence of ac susceptibility in $Ni_{54}Fe_{19}Ga_{27}$ sample*

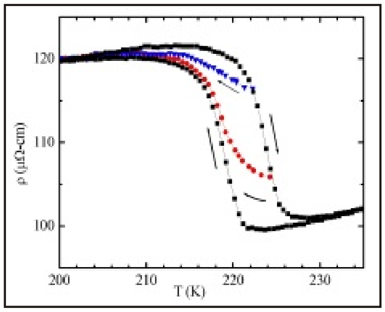

***Fig. A.5.2** Thermal hysteresis in the resistivity data of $Ni_{54}Fe_{19}Ga_{27}$ sample around the MT.*
The figure also depicts minor hysteresis loops.

MT occurs through nucleation and growth. Upon cooling, martensite starts to develop from a temperature M_s and the growth finishes at M_f. Similarly, while heating, A_s and A_f denote austenite start and finish temperatures respectively. In order to understand the irreversible region of first order transition, we have performed a careful resistivity investigation across the MT. The region of irreversibility begins at A_f = 231 K and it closes at M_f = 198 K. Minor hysteresis loops (MHL) have been recorded between temperatures A_f and M_f by reversing the direction of heating/cooling. The resistivity data traces a different path as compared to full heating-cooling envelope curve (fig. A.5.2). The existence of distinct MHL indicate that both martensite and austenite phases can coexist in the region of irreversibility. On the heating envelope curve MHL starts to develop from A_s = 209 K, while on the cooling envelope MHL exist below M_s = 225 K, which constitute the boundaries for the region of phase coexistence. The observed thermal hysteresis and minor hysteresis loops support first order nature of the transition along with the phase coexistence in the irreversible region.

(Contributed by: S. Majumdar; subham@cat.ernet.in and V. K. Sharma)

A.6 Optical design of XRF microprobe beam line on Indus-2

Microprobe X-ray fluorescence (μ-XRF) and X-ray fluorescence (XRF) are powerful tools for determination of elemental heterogeneity and elemental composition of materials. With synchrotron radiation as the source, the sensitivity of these techniques can improve considerably. It is proposed to install a XRF microprobe beam-line on Indus-2. The basic applications are micro mapping of elemental heterogeneity and trace element analysis. Optical design of the beam line is completed.[CAT 2005-10]. The optical layout is given in fig. A.6.1.

Obtaining small spot size with maximum flux at the sample position has been the principal design consideration in this beam line. Apart from this, controllable energy resolution and spot size are other two principal features of the beam line. The objectives have been achieved by using asymmetrically cut Si (111) double crystal monochromator as dispersive optics and Kirkpatrick Baez (KB) mirror pair as focusing optics. The ray tracing simulations of the described design yield spot size of approximately 2μm (H) × 9μm (V) (fig. A.6.2) with ~ 10^8 photons/sec and energy resolution (E/DE) ~1000 at 10 keV photon energy. The beam line will operate in 3-20 keV photon energy range. The lower energy limit is defined by transmission through Be window and air where as the upper energy limit is defined by the cut off energy of the Pt coating of the mirrors of KB mirror system.

The first crystal of the monochromator will have -5^0 asymmetric angle with (111) plane of silicon, and the second crystal will have 5^0 asymmetric angle. Because of greater incident rocking curve width of the first crystal, the monochromator will pass higher flux compared to symmetric cut crystal monochromator. A slit before the first crystal of the monochromator will control the energy resolution of the beam line. With a controlled slit opening, the beam line can provide (E/DE) ~ 10,000 which is suitable for X-ray absorption spectroscopy, and total reflection X-ray fluorescence class of experiments. When the slit is wide open to allow the whole vertical divergence, the beam line can provide ~ 10^{10} photons/sec on a spot of size 20mm(H)×5mm(V) in unfocused mode.

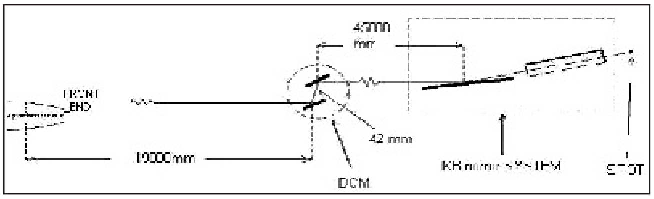

Fig. A.6.1 *Optical design of the XRF microprobe beam line on Indus- 2*

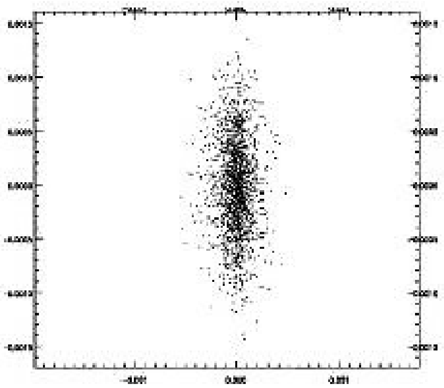

Fig. A.6.2 *Spot on the sample*

Two elliptical mirrors in KB arrangement focus the beam in vertical and horizontal direction. The mirrors are platinum coated and operate at grazing angle of 3.9 milliard. The horizontal and vertical acceptance of the beam line is defined by the acceptance of the 1st and 2nd mirror which is ~ 30 mrad. Both the mirrors can be removed to provide unfocused beam, which can be collimated to required size by high precision slits. The parameters of the second mirror can be changed to get a required spot size. Also the second mirror can be removed from the beam path to get vertically focused beam whose horizontal size can be controlled by high precision slits.